

# RSC Advances



This is an *Accepted Manuscript*, which has been through the Royal Society of Chemistry peer review process and has been accepted for publication.

*Accepted Manuscripts* are published online shortly after acceptance, before technical editing, formatting and proof reading. Using this free service, authors can make their results available to the community, in citable form, before we publish the edited article. This *Accepted Manuscript* will be replaced by the edited, formatted and paginated article as soon as this is available.

You can find more information about *Accepted Manuscripts* in the [Information for Authors](#).

Please note that technical editing may introduce minor changes to the text and/or graphics, which may alter content. The journal's standard [Terms & Conditions](#) and the [Ethical guidelines](#) still apply. In no event shall the Royal Society of Chemistry be held responsible for any errors or omissions in this *Accepted Manuscript* or any consequences arising from the use of any information it contains.



## Honeycomb-shaped magnetic multilayer thin films for cell trapping

Received 00th January 20xx,  
Accepted 00th January 20xx

DOI: 10.1039/x0xx00000x

[www.rsc.org/](http://www.rsc.org/)

Chen-Yu Huang,<sup>a†</sup> Wei-Chieh Chang,<sup>b†</sup> Kun-Chieh Yeh,<sup>c†</sup> Han-Yi Tseng,<sup>de</sup> Ming-Shinn Hsu,<sup>ftt</sup> Jiann-Yeu Chen,<sup>g††</sup> Zung-Hang Wei<sup>a††</sup>

Honeycomb-shaped magnetic thin films with domain wall (DW) pinning geometry are designed to actively trap magnetically labeled cells. After an initial in-plane magnetic field ( $H_{\text{initial}}$ ) is applied and later reduced to zero, the resultant magnetization became locally aligned. Human hepatocellular liver carcinoma cell line (HepG2) stably expressed green fluorescent protein (GFP) are magnetically labeled with superparamagnetic magnetic nanoparticles (MNPs). Prussian blue stain and single cell magnetophoresis are performed to evaluate the internalization of the MNPs. Magnetically labeled cells are then trapped by the stray fields of head-to-head DWs (HH DWs) or tail-to-tail DWs (TT DWs). After co-cultured with magnetic structure, HepG2 cells stretched out and showed filopodia-like protrusions to contact with adjacent cells.

### Introduction

Cell manipulation techniques have aroused considerable attention in the field of biomedical research. For instances, cell-based assays,<sup>1</sup> homotypic/heterotypic cell-cell interaction,<sup>2</sup> tissue engineering<sup>3</sup> and so on. A conceptual idea for cell manipulation that proposed by Carter *et al.* as early as 1965,<sup>4</sup> make use of unique features to control cell distribution, influence cell morphology as well as modulate cell function. Later, approaches adopt different mechanisms to manipulate cells; some of them distributed biomolecules on chips for cells to adhere selectively to particular positions,<sup>5-7</sup> while others actively move cells by external forces to the designated area. The techniques to actively pattern cell in micron scale involved the use of microfluidic flow,<sup>8</sup> magnetic,<sup>9-11</sup> electric,<sup>12</sup> optical,<sup>13</sup> and acoustic force<sup>14</sup> or the combination.<sup>15</sup> Specifically, experiments based on the magnetic force have merits such as non-contact, contamination-free or low adverse effects on

biological entities which make them to the biomedical field. Literature revealed that the magnetization of soft ferromagnetic materials with high shape anisotropy are inclined to orient parallel to the boundary structure to reduce the magnetostatic energy.<sup>16</sup> For a magnetic thin film with network structures, the magnetization of each junction arm are rather stable and produce local stray fields,<sup>17</sup> which offers the opportunity to control the location of magnetically labeled cells. Therefore, based on this concept, the study designed honeycomb-shaped magnetic structures to actively trap and pattern cells. Cells were stably expressed green fluorescent protein (GFP) and magnetically labeled with superparamagnetic magnetic nanoparticles (MNPs). Furthermore, cell were co-cultured with the structure after trapped by the local stray fields. Cell morphology were found to be influenced by the geometry and topography of the honeycomb magnetic structure.

### Experimental procedures

#### Magnetic thin film structures fabrication

Glass substrates were spin-coated with a layer of photoresistor (AZ4621, AZ Electronic Materials) and then followed by photolithography and e-beam evaporation process. The deposition process involving repeated deposition of 10 nm of titanium (Ti) as an adhesion layer and then 30 nm of iron (Fe) for a total of 5 cycles. 10 nm of titanium (Ti) was covered to protect the sample from oxidation. Finally, samples were submerged into acetone to lift-off unwanted metals and then about 100 nm of Poly(methyl methacrylate) (PMMA) was spin coated to cover the entire surface and baking at 80 °C. The top layer PMMA not only protected the thin films from oxidation as exposed to air or liquid solution but also prevented the biological cells from direct contacting with magnetic films and

<sup>a</sup> Department of Power Mechanical Engineering, National Tsing Hua University, Hsinchu City, Taiwan

<sup>b</sup> Department of Neurosurgery, Show Chwan Memorial Hospital, Changhua, Taiwan

<sup>c</sup> Department of Surgery, Taoyuan Armed Forces General Hospital, Taoyuan, Taiwan

<sup>d</sup> Department of Ophthalmology, Kaohsiung Medical University Hospital, Kaohsiung Medical University, Kaohsiung, Taiwan

<sup>e</sup> Department of Ophthalmology, Kaohsiung Municipal Hsiao-Kang Hospital, Kaohsiung Medical University, Kaohsiung, Taiwan

<sup>f</sup> Department of Obstetrics and Gynecology, Ching-Kuo Campus of Min-Sheng Hospital, Taoyuan, Taiwan

<sup>g</sup> Center of Nanoscience and Nanotechnology, National Chung Hsing University, Taichung, Taiwan

<sup>†</sup> The authors contribute equally in this paper.

<sup>††</sup> Co-corresponding authors.

Electronic Supplementary Information (ESI) available: [details of any supplementary information available should be included here]. See DOI: 10.1039/x0xx00000x

inducing toxicity effects. The aspect ratio of the line width of the structure is designed to assure the uniformity of the magnetization.

#### Cell culture and green fluorescent protein (GFP) gene transfection

Human hepatocellular carcinoma cell lines, HepG2 (BCRC No. 60025) were purchased from the Bioresources Collection and Research Center (BCRC) of the Food Industry Research and Development Institute (Hsinchu, Taiwan). Cells were grown in DMEM with high glucose supplemented with 10% heat-inactivated fetal bovine serum at 37 °C and maintained in 5% CO<sub>2</sub> environment with humidified atmosphere. The pre-made lentivirus particles (pAS7w.EGFP.puro) were obtained from the National RNAi Core Facility, Institute of Molecular Biology/Genome Research Centre, Academia Sinica, Taipei, Taiwan. While grown to 80~90% confluence, cells were infected with lentiviruses at a multiplicity of infections (MOIs) of 3 in complete medium containing polybrene of 8 µg/ml and incubated for 24 h. GFP signal was examined by inverted fluorescence microscopy at two days post-infection, and GFP-positive cells were isolated by puromycin purchased from Sigma-Aldrich for two weeks at an optimized concentration of 1 µg/ml.

#### Magnetic labeling process

Before magnetic labeling, cells were seeded at a concentration of 10<sup>5</sup> cells/well in 12-well culture plates to reach 90% confluence. After that, cells were incubated with MNPs (Water-Based Ferrofluids, WEISTRON Co., Ltd.) in DMEM medium at the concentration of 1 µg/ml and washed three times by replacing with fresh PBS to remove nonspecific bounded MNPs. Consequently, the cells were concentrated by a permanent magnet that placed on the outer wall of the centrifuge tube and were resuspended in fresh culture medium.

#### Quantification of internalized nanoparticle by single cell magnetophoresis

The experimental procedures and setups for single cell magnetophoresis were previously reported.<sup>18</sup> Briefly, the magnetically labeled HepG2 cells suspended in DMEM medium were exposed to a constant magnetic field gradient ( $\text{dB}/\text{dx}=14 \text{ mT}/\text{mm}$ ) generated by a permanent magnet. As the magnetic force exerted by the magnetic moment of the total MNPs inside cells ( $m_{\text{cell}}$ ),  $F_m = m_{\text{cell}} \text{dB}/\text{dx}$ , was balanced by the drag force,  $F_d = 6\pi\eta R_{\text{cell}} v_{\text{cell}}$ , that opposed the motion, the number of MNPs  $N$  inside a cell could be calculated by  $N = (36\eta R_{\text{cell}} v_{\text{cell}}) / (cM_s D_{\text{TEM}}^3 \text{dB}/\text{dx})$ .  $R_{\text{cell}}$  (10 µm) is the radius of cell,  $\eta$  is the viscosity of the carrier liquid,  $v_{\text{cell}}$  is the cell velocity,  $D_{\text{TEM}}$  (9.93 nm) is the diameter of MNPs, and  $c$  is the ratio of net magnetization of MNPs to their saturation magnetization  $M_s$  (=0.8).

#### Prussian blue stain

HepG2 cells were stained with Prussian blue stain to directly visualize the localizations of iron oxide MNPs. Both magnetically labeled cells and controls (without labeling)

were incubated in 4% glutaraldehyde (GA) for 30 min at -20 °C to be fixed. Prussian blue staining reagent including the mixture of 2% potassium ferrocyanide and 6% HCl (1/1, v/v) was incubated with cells for 20 min and followed by counterstaining with nuclear fast red to visualize cell nuclei.

#### Equipment and image analysis

Cells transfected by GFP lentivirus were visualized by a fluorescence microscope (Olympus CKX41) equipped with blue, green and UV filters. The moving cells that were attracted by the local magnetic force generated by DWs were recorded with a CCD camera for 15-20 min at five frames per second. The image sequences were then imported into the open source software, ImageJ, and the displacements of each cell were tracked via the plug-in "manual tracking". The diameter of cells was investigated by analyzing the photos of cells through the built-in measurement tool of Mshot Digital Imaging System.

#### Transmission electron microscope (TEM) and particle size measurement

The particles were examined using a transmission electron microscope (Hitachi HT7700TEM) and a total of about 200 particles from TEM images were analyzed to obtain particle size. The size distribution could be fitted using the log-normal function, where the characteristic diameter  $D_0$  and the polydispersity parameter (or standard deviation)  $\sigma$  can be obtained. Probability density  $P(D)$  can be used to get the characteristic diameter  $D_0$  and the polydispersity parameter (or standard deviation)  $\sigma$  can be written as:

$$P(D) = 1/\sqrt{2\pi\sigma D} \exp\{[\ln D/D_0]^2/2\sigma^2\}$$

the respective value of  $D_0$  and  $\sigma$  are found to be 9.78 nm and 0.18 from size distribution obtained from TEM images. The

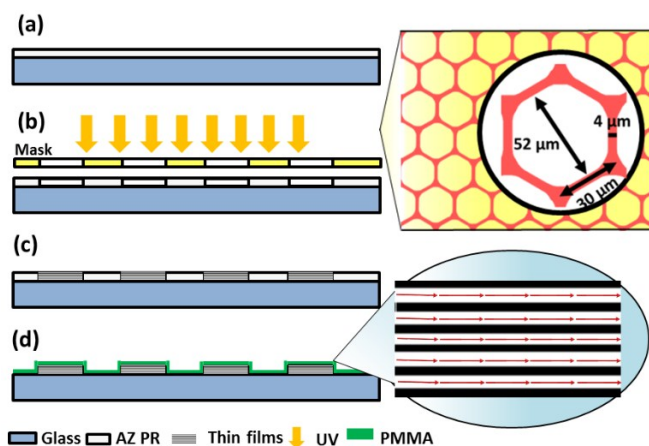


Figure 1. Honeycomb-shaped magnetic thin films fabrication process. (a) spin-coating a layer of photoresist on glass (b) UV light exposure (c) thin film deposition of Fe/Ti multilayer (d) lift-off unwanted metal. Separate stacked thin film layers that each consist of magnetic layer spaced with non-magnetic layer ensures the homogeneity of Néel walls throughout the element.

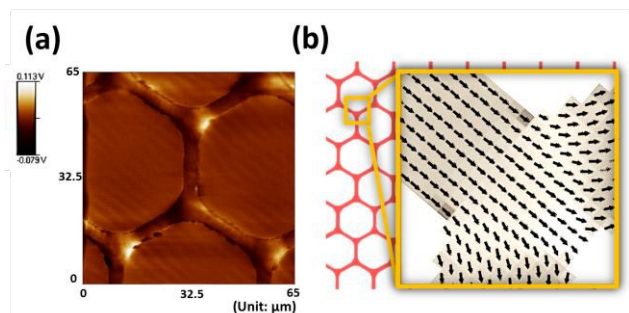


Figure 2. (a) MFM image of the honeycomb-shaped magnetic structure after an in-plane magnetic field ( $H_{\text{initial}}$ ) was applied to saturate the magnetization. (b) The central part of the spin configurations of the three-arm junctions of honeycomb. The arrows indicate the magnetization vectors while the grayscale indicates the magnetic pole densities.

average size  $D_{\text{TEM}}$  can then be estimated by taking polydispersity  $\sigma$  into account,  $D_{\text{TEM}} = D_0 \exp(\sigma^2/2)$ , which is 9.93 nm.

## Results and discussion

Photolithography and e-beam evaporation were used to prepare the honeycomb-shaped magnetic thin film structure, as shown in Figure 1. To ensure the homogeneity of  $N'ee'$  walls throughout the element, multilayer thin films that consists of magnetic layers spaced with non-magnetic layers were used.<sup>19</sup> To create stable magnetic states in the geometry, the honeycomb-shaped structures were subjected to an external magnetic field (3000 Oe) in the in-plane direction to saturate the magnetization initially ( $H_{\text{initial}}$ ) and then the magnetic field

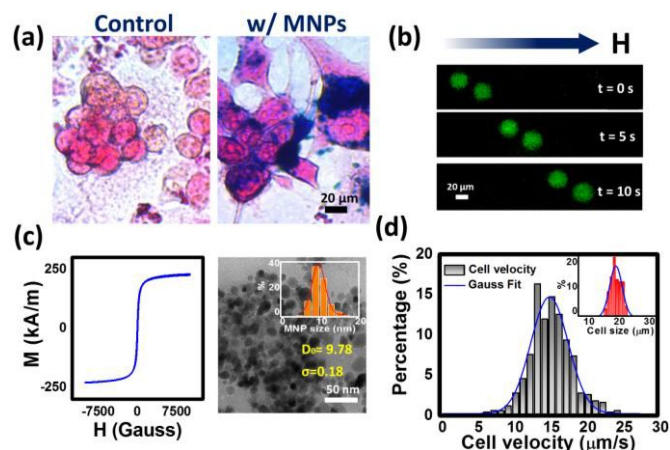


Figure 3. (a) Optical microscopy images of Prussian blue staining of HepG2 cells that were not incubated with MNPs (control) and cells magnetically labeled with MNPs (w/ MNPs). (b) GFP-expressed cell perform magnetophoresis. H: external magnetic field. (c) The magnetization versus magnetizing field curve (M-H curve) of magnetic nanoparticles and TEM picture with MNP size distribution (d) the velocity distribution for single cell magnetophoresis analysis of the internalized nanoparticle number. Inset: the size of cells.

gradually receded towards zero. The domain configurations of the magnetic structure in the remanent state could later be confirmed by the magnetic force microscopy (MFM) image, as shown in Figure 2a. The magnetic configuration can be described in Figure 2b, which displays the magnetization vectors in one arm point into the center of the junction while those in the other two arms point outwards. As previously described by Lai *et al.*, the resultant magnetization is the one with the lowest energy density.<sup>17</sup> Besides, as found by Pushp *et al.* that the remnant state honeycomb network would appear broken symmetries such as head-to-head (HH) and tail-to-tail (TT) DWs, and, therefore, generated local stray field to be sensed by MFM probe.<sup>20</sup>

Human hepatocellular carcinoma cell lines (HepG2) were magnetically labeled via internalization of MNPs. After Prussian blue staining, cells labeled by MNPs showed blue deposits in the cytoplasm while control cells did not (Figure 3a). The consecutive images of GFP-expressed cells performing magnetophoresis are illustrated in figure 3b. Since only cells remain alive can express GFP, the expression of fluorescence enabled us to verify the cell viability before and after cell trapping. The number of MNPs was quantified by obtaining constant velocity ( $v_{\text{cell}}$ ) from single cell magnetophoresis. The average value of  $v_{\text{cell}}$  was  $15.37 \pm 3.002 \mu\text{m/s}$ , which shows a Gaussian distribution (Figure 3d). By obtaining the average MNPs size ( $D_{\text{TEM}} = 9.93 \text{ nm}$ ) from TEM images (Figure 3c), cell radius ( $R_{\text{cell}}$ ) of  $10 \mu\text{m}$  from Figure 3d, the number of MNPs in each cell could be estimated to be  $(2.15 \pm 0.42) \times 10^6/\text{cell}$ , which is equal to  $5.44 \pm 1.062 \text{ pg iron/cell}$ .

The HH DWs and TT DWs, which show single magnetic pole characteristics and act like small magnets to generate local magnetic stray fields, can attract magnetic entities. As seen in

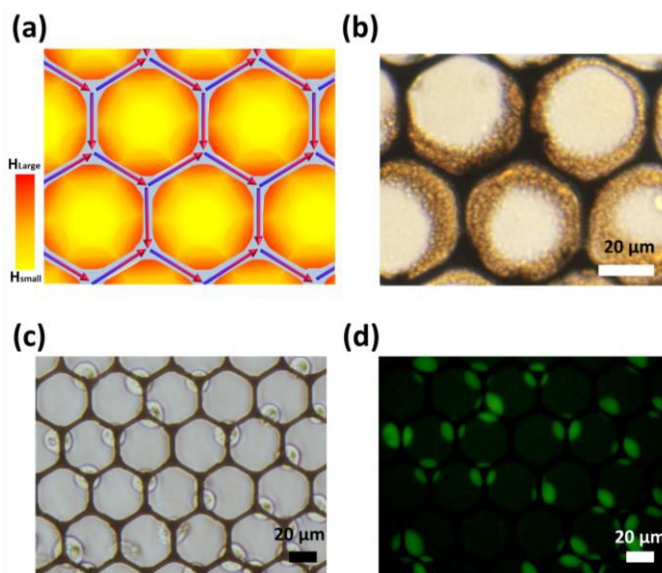


Figure 4. (a) Illustration of magnetization configuration and local magnetic stray field distribution (b) coffee ring structure formed by magnetic nanoparticles attracted by the stray fields generated by DWs (c) Optical images and (d) fluorescence image of GFP-expressed HepG2 cells attracted and arranged at the vertices of the magnetized honeycomb structure. Cell concentration =  $5 \times 10^5 \text{ cells/mL}$ .

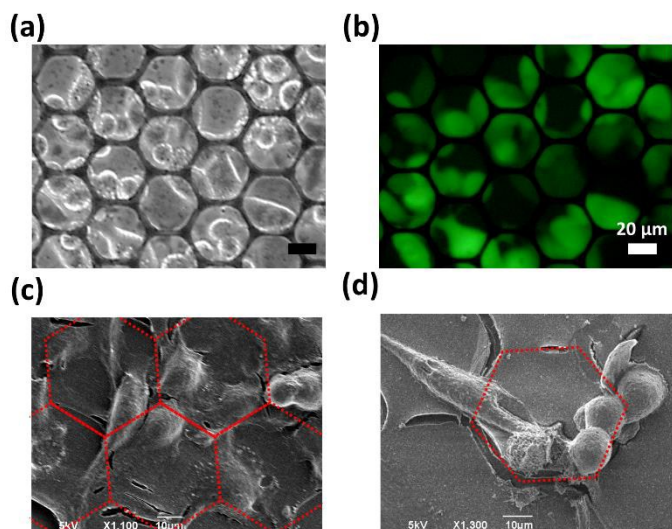


Figure 5. Optical microscope/fluorescence/SEM images of HepG2 cells grew on honeycomb structures. (a) and (b) show viable cells expressed green fluorescence protein (GFP) and grew on the structure. (c) and (d) SEM images reveal microstructures of HepG2 cells.

Figure 4a, the strength of the local magnetic field of the honeycomb-shaped structure is strongest near the junction of arms where DWs produced. Therefore, MNPs could be attracted and collected to form “coffee ring” like patterns as a consequence (Figure 4b). The honeycomb structures were then utilized for trapping cells, and the results were taken by a fluorescence microscope, as shown in Figure 4c and 4d. After magnetic structures magnetized by  $H_{\text{initial}}$  and released from the field, the GFP-expressed HepG2 cells were trapped by the local magnetic stray fields in the vicinity of HH/TT DWs. After most of the cells have been trapped by DWs, the residual suspension was slowly rinsed off and replaced by fresh medium. The trapped HepG2 cells were then kept cultured with the structure for two days. As seen in Figure 5a and 5b, cells grew on the structure remaining viable and expressed green fluorescence protein (GFP). The morphology of cells was then analyzed by SEM, as seen in Figure 5c and 5d. Some cells grew on the honeycomb structure remain rounded, while others stretched out appearing filopodia-like protrusions, elongated to contact with adjacent cells and grew along the honeycomb-shaped structures. As proposed by previous literature,<sup>21</sup> such cell morphology influenced by the surface topographical features of magnetic thin films may be caused by the contact guidance alignment.<sup>22</sup>

In this study, the concept of micromagnetism of patterned multilayer thin films has been utilized to generate stable DWs. We have thoroughly analyzed its micromagnetic property and demonstrated its stability for manipulating biological cells. Previously, such patterned magnetic structures have shown thermal stability to avoid the superparamagnetic limit,<sup>23</sup> and have been used for data storage media to decrease the noise during information accessing.<sup>24</sup> Recently, selective manipulation of target cells from bulk solutions and enrich cells into population to provide insight information of disease state is in need.<sup>25-27</sup> The proposed magnetic structures

designed for biological manipulations are easy to fabricate. Besides, they do not require additional external magnetic force after having been magnetized, which are energy efficient. These advantages make the proposed structures suitable for future biological chip applications.

## Conclusions

Honeycomb magnetic thin films with DW pinning geometry were utilized to trap magnetically labeled cells. The local magnetic force produced by the magnetic DWs in the remnant state can attract cells to the specific positions. This energy saving strategy can be ideally for future isolation or separation applications.

## Acknowledgements

This work is supported partly by the Ministry of Science and Technology (MOST), Taiwan grant numbers MOST 102-2112-M-007-012-MY3, MOST 103-2221-E-007-017-MY2, MOST 104-2221-E-007-015-MY4.

## References

- 1 S. Juul, Y. P. Ho, J. Koch, F. F. Andersen, M. Stougaard, K. W. Leong, and B. R. Knudsen, *ACS Nano*, 2011, **5**, 8305.
- 2 F. Guo, P. Li, J. B. French, Z. Mao, H. Zhao, S. Li, N. Nama, J. R. Fick, S. J. Benkovic, and T. J. Huang, *Proc. Natl. Acad. Sci. U.S.A.*, 2015, **112**, 43.
- 3 S. V. Murphy and A. Atala, *Nature Biotechnol.*, 2014, **32**, 773.
- 4 S. B. Carter, *Nature*, 1965, **208**, 1183.
- 5 K. A. Mosiewicz, L. Kolb, A. J. van der Vlies, M. M. Martino, P. S. Lienemann, J. A. Hubbell, M. Ehrbar, and M. P. Lutolf, *Nat. Mater.*, 2013, **12**, 1072.
- 6 S. G. Ricoult, G. Thompson-Steckel, J. P. Correia, T. E. Kennedy, and D. Juncker, *Biomaterials*, 2014, **35**, 727.
- 7 S. Joo, J. Y. Kim, E. Lee, N. Hong, W. Sun, and Y. Nam, *Sci. Rep.*, 2015, **5**, 13043.
- 8 L. Lin, Y. S. Chu, J. P. Thiery, C. T. Lim, and I. Rodriguez, *Lab Chip*, 2013, **13**, 714.
- 9 M. F. Lai, C. Y. Chen, C. P. Lee, H. T. Huang, T. R. Ger and Z. H. Wei, *Appl. Phys. Lett.*, 2010, **96**, 183701.
- 10 C. Y. Huang, Z. H. Wei, *PLoS ONE*, 2015, **10**, e0135299.
- 11 C. Y. Huang, M. F. Lai, T. R. Ger, and Z. H. Wei, *J. Appl. Phys.*, 2015, **117**, 17B309.
- 12 S. Prasad, X. Zhang, M. Yang, Y. Ni, V. Parpura, C. S. Ozkan, and M. Ozkan, *J. Neurosci. Methods*, 2004, **135**, 79.
- 13 P. Y. Chiou, A. T. Ohta, and M. C. Wu, *Nature*, 2005, **436**, 370.
- 14 F. Gesellchen, A. L. Bernassau, T. Déjardin, D. R. S. Cumming and M. O. Riehle, *Lab Chip*, 2014, **14**, 2266.
- 15 N. Erdman, L. Schmidt, W. Qin, X. Yang, Y. Lin, M. N. DeSilva, and B. Z. Gao, *Biofabrication*, 2014, **6**, 035025.
- 16 M. F. Lai, Z. H. Wei, C. R. Chang, J. C. Wu, J. H. Kuo, and J. Y. Lai, *Phys. Rev. B.*, 2013, **87**, 104419.
- 17 M. F. Lai, Z. H. Wei, J. C. Wu, C. R. Chang; N. A. Usov, Ida Chang, and J. Y. Lai, *IEEE Trans. Magn.*, 2005, **41**, 953.
- 18 C. Y. Huang, T. R. Ger, Z. H. Wei, and M. F. Lai, *PLoS ONE*, 2014, **9**, e96550.
- 19 M. T. Johnson, P. J. H. Bloemen, F. J. A. den Broeder, and J. J. de Vries, *Rep. Prog. Phys.*, 1996, **59**, 1409.
- 20 A. Pushp, T. Phung, C. Rettner, B. P. Hughes, S. H. Yang, L. Thomas, and S. S. P. Parkin, *Nature Phys.*, 2013, **9**, 505.

- 21 E. Eisenbarth, J. Meyle, W. Nachtigall, and J. Breme, *Biomaterials*, 1996, **17**, 1399.
- 22 S. A. Biela, Y. Su, J. P. Spatz, and R. Kemkemer, *Acta Biomater.*, 2009, **5**, 2460.
- 23 J. G. Zhu and H. Fang, *IEEE Trans. Magn.*, 1998, **34**, 1609.
- 24 L. Torres, L. Lopez-Diaz, and J. Iñiguez, *Appl. Phys. Lett.*, 1998, **73**, 3766.
- 25 S. Braun and C. Marth, *N. Engl. J. Med.*, 2004, **351**, 824.
- 26 H. J. Kahn, A. Presta, L.-Y. Yang, J. Blondal, M. Trudeau, L. Lickley, C. Holloway, D. R. McCready, D. Maclean, and A. Marks, *Breast Cancer Res. Treat.*, 2004, **86**, 237.
- 27 S. Nagrath, L. V. Sequist, S. Maheswaran, D. W. Bell, D. Irimia, L. Ulkus, M. R. Smith, E. L. Kwak, S. Digumarthy, A. Muzikansky, P. Ryan, U. J. Balis, R. G. Tompkins, D. A. Haber, and M. Toner, *Nature*, 2007, **450**, 1235.